

Supplement of Earth Syst. Dynam. Discuss., 5, 809–848, 2014
<http://www.earth-syst-dynam-discuss.net/5/809/2014/>
doi:10.5194/esdd-5-809-2014-supplement
© Author(s) 2014. CC Attribution 3.0 License.



Supplement of

**Temporal variations in atmospheric CO₂ on Rishiri Island in 2006–2013:
responses of the interannual variation in amplitude to climate and the
terrestrial sink in East Asia**

C. Zhu and H. Yoshikawa-Inoue

Correspondence to: C. Zhu (chmzhu@pop.lowtem.hokudai.ac.jp)

Supplementary materials

This file includes:

Details on data selection and curve fitting

Table S1

Figs. S1 to S7

References

Details on data selection and curve fitting

In this section, the procedures to extract seasonal cycle and secular trend will be described. A selection criterion for the continuous hourly data was first applied. Hours of the day representing long-range transport were then selected to calculate daily means. The seasonal and long-term trends were then extracted based on the daily means using function fit and digital filtering approaches.

1. Hourly data selection

For the observed records, large variations in the consecutive hours were caused by local phenomenon. A homogeneous air mass free of local contamination had small within-the-hour and hour-to-hour CO₂ concentration variations (Peterson et al., 1982). In this step, the aim was to remove hours where the variation in continuous CO₂ concentration was larger than a specific value. In previous studies, several protocols have been used to select data representing large-scale phenomena. Peterson et al. (1982, 1986) considered that if the difference between consecutive hours was larger than 0.25 ppm, both of those hours should be rejected. However, in summer months with large hourly variability, this strict selection criterion would remove the majority of the data and result in the loss of essential information. Thoning et al. (1989) thereafter adopted a modified criterion where if any two consecutive values differed by less than the 0.25 ppm, the data were retained. Recently, Brailsford et al. (2012) proposed that the data should be kept only if the standard deviation over a 6-hour period was no more than 0.1 ppm.

In this study, the data continuity after applying hour-to-hour variation for the criteria used by Peterson et al. (1982) and Thoning et al. (1989) was examined. Thresholds at 0.25 ppm, 0.5 ppm and 1 ppm were compared (Fig. S1). In Figure S1, panels a, c and e indicated the hour-to-hour variation of CO₂ records when any two consecutive values differed by less than the threshold (Thoning et al., 1989). This was called the “single-side” selection criterion. Panels b, d and f were the selected data when the differences between both consecutive hours were less than the threshold. This was called the “two-side” selection criterion. After selection, the percentages of remaining data to the original record were 47.4%, 63.2% and 77.0% in the 0.25 ppm, 0.50 ppm and 1 ppm threshold for the single-side criterion, and 19.6%, 36.3% and 54.7% in the 0.25 ppm, 0.50 ppm and 1 ppm threshold for the two-side criterion, respectively.

Investigation on the post-selected datasets showed that the 0.25 ppm threshold for the two-side criterion, which is the strictest selection, lost the signals in summer months. For example, in the summer of 2008, most of the records were lost from July to the middle of September. Similar information lost also appeared for the 0.50 ppm threshold for the two-side criterion. For the 1 ppm threshold, although it kept most of the information, the hourly variation up to 1 ppm might also be affected by the local sources/sinks. As a result, the 0.25 ppm threshold with the single-side criterion was used, which was also used by Thoning et al. (1989) for the analysis of Mauna Loa data.

2. Representative hours of the day

As a marked diurnal variation appeared in the summer months, the second step for data selection was to choose hourly data of the day that represents the least local influence. Based on the diurnal variation pattern (Fig. S2), the dataset including daytime hours (1000–1500 LT), nighttime hours (2200–0300 LT), the transition hours (0500–0700 and 1700–1900 LT), and the unselected whole hours of a day were compared. After this step selection, the percentages of remaining data to the original record were 14.1% for the daytime hours, 11.3% for the nighttime hours, 10.7% for the transition hours, and 47.4% for the unselected whole hours of a day. The daily means calculated based on these datasets are plotted in Figure 3.5. It could be clearly observed that the daily means based on daytime hours had the lowest noise level, while

the baseline representing large-scale influences was apparent. This was mainly attributed to the maritime and long-range origins of air masses. For the nighttime derived dataset, a large noise level existed so that it was difficult to see the baseline, especially in the summer months. This was caused by the formation of stable nocturnal inversions, as discussed above. The transition hours were also examined for the possibility of representativeness of air masses from far regions. However, the daily means based on this dataset were quite scattered and unable to catch the baseline. The dataset of the whole day hours, having a reasonable baseline pattern and moderate noise levels, incorporated both local and large-scale phenomenon.

To investigate the magnitudes of the differences between these four datasets, the mean concentrations over 2006–2013 were calculated as the simple arithmetic means. The results indicated that the daily means based on the daytime hours, nighttime hours, transition hours and the whole day hours were 391.0 ppm, 395.9 ppm, 394.2 ppm and 392.5 ppm, respectively. The dataset based on the daytime hours had the lowest value, and that based on nighttime hours had the highest one. The results implied that the datasets except for the daytime hours are incorporating quite a large amount of local contributions. Therefore, in the following analysis, the daily means based on daytime hours (1000–1500 LT) were chosen to examine large-scale variations.

There have been arguments that the data could also be selected based on local meteorology such as the removal of calm hours (Haszpra, 1999). With the currently used approach, the calm hours (wind speed $\leq 0.2 \text{ m s}^{-1}$) were almost completely removed. As in 2011, only one calm hour was kept after applying these two steps of selection.

3. Applying the function fit and filtering the residuals

To extract the seasonal and long-term trends, curve fittings consisting of function fit to the daily means and filtering to the residuals from the fit were applied (Thoning et al., 1989). The function fit included polynomial terms and harmonic terms, as shown in equation 1,

$$x(t) = c + dt + et^2 + ft^3 + \sum_{i=1}^3 \left[a_i \cos\left(\frac{2\pi}{T} it\right) + b_i \sin\left(\frac{2\pi}{T} it\right) \right] \quad (1).$$

In the equation, t was the day count, and T was equal to 365 days. The calculated fit (preliminary) is shown in Figure S3a. This fit, however, did not include enough information of the seasonal and interannual variations. The data were then calculated for the residuals of the daily means about the function fit (Fig. S3b). Low-pass filters were thereafter applied to the residuals. This application requires that the data be equally spaced with no gaps. Linear interpolation was applied to the residuals to fill the missing gaps. When applying the low-pass filter, cutoff frequencies of 120 days for the short-term and 667 days for the long-term variations were used. The filtered residuals are also plotted in Figure S3b. In the last step, the function fit was adjusted by adding the short-term filtered residuals (Fig. 4a). Meanwhile, a combination of the polynomial and the long-term filtered residuals constituted the long-term trend (Fig. 4a). The de-trended seasonal cycle, namely the annual oscillation, was thereafter separated by removing the long-term trend from the smoothed fit (Fig. 4b). The growth rate was obtained as the derivative of the long-term trend (Fig. 4b).

Using the approach described by Thoning et al. (1989), the statistical uncertainties were estimated for the components of the estimation. The standard deviation of the residuals about the preliminary fit was 3.43 ppm. For the short-term filter (cutoff frequency 120 days), the standard deviation was estimated as 0.40 ppm. For the long-term filter (cutoff frequency 667 days), the standard deviation was estimated as 0.17 ppm. After applying the low-pass filter, the residuals about smoothed fit (seasonal cycle) were 3.28 ppm. For the smoothed seasonal cycle, the standard deviation was estimated to be 0.40 ppm. For the long-term trend, the standard deviation was estimated to be 0.19 ppm. For the de-trended cycle, the standard deviation was estimated as 0.44 ppm. A standard deviation of 0.27 ppm yr^{-1} was estimated for the growth rate.

Table S1. Linear correlation coefficients (R^2) between amplitude anomalies at Rishiri Island and anomalies of temperature and precipitation in East Asia (EA), broad East Asia (BEA), the Northern Hemisphere (NH) and the global (GL) in 2006–2013.

Period ^a	with temperature anomalies				with precipitation anomalies			
	EA	BEA	NH	GL	EA	BEA	NH	GL
Current year ^b	-0.19	-0.17	0.12	0.02	-0.03	-0.24	-0.18	-0.19
Apr-Mar	-0.12	-0.14	0.08	0.10	-0.20	0.13	-0.12	-0.04
Oct-Mar	-0.18	-0.17	-0.20	-0.20	-0.20	-0.02	-0.16	-0.02
Mar	-0.18	-0.17	-0.19	-0.14	0.21	0.26	-0.08	-0.01
Aug-Mar	-0.17	-0.16	-0.17	-0.17	-0.19	0.02	-0.11	0.01
Sep-Aug	-0.25	-0.24	0.17	0.004	-0.18	-0.15	0.07	-0.02
Mar-Aug	-0.22	-0.14	0.39	0.17	-0.12	-0.19	-0.13	-0.16
Jun-Aug	0.20	0.14	0.21	0.02	-0.08	-0.19	-0.17	-0.19
Aug	0.11	0.15	0.12	-0.01	-0.19	0.24	0.31	0.23

^a Except for “Current year”, temperature and precipitation anomalies are calculated in each of the periods counted in reverse from the end of the month to the month in the previous year; see text for details.

^b Correlations are amplitude anomalies with temperature and precipitation anomalies of the same year (January to December).

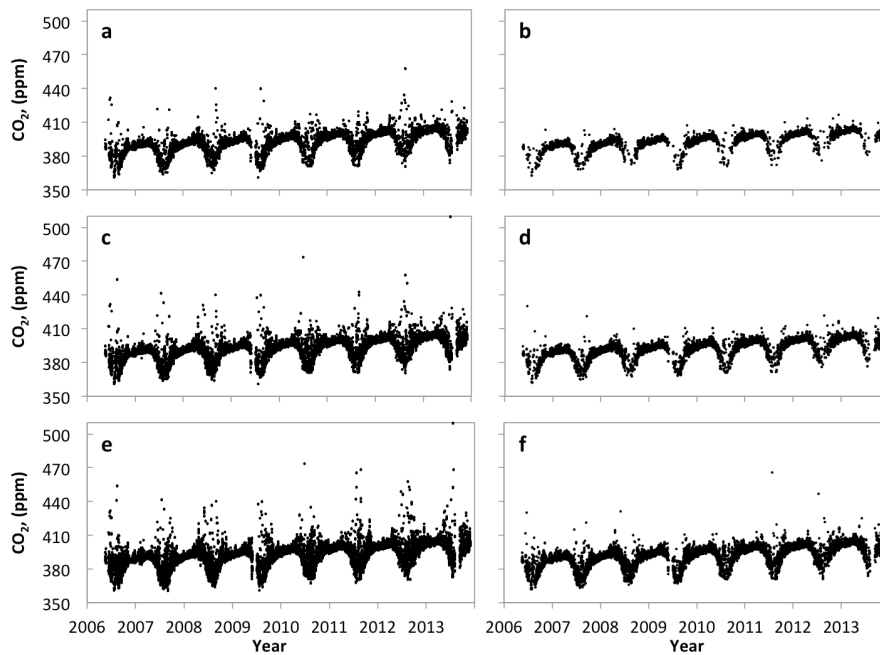


Fig. S1. Selected hourly data after applying different criteria to the original observed record. Panels a, c and e show the selected data when any two consecutive hourly variations are less than 0.25 ppm, 0.5 ppm and 1 ppm, respectively, and panels b, d and f show the selected data when both consecutive hourly variations are less than 0.25 ppm, 0.5 ppm and 1 ppm, respectively.

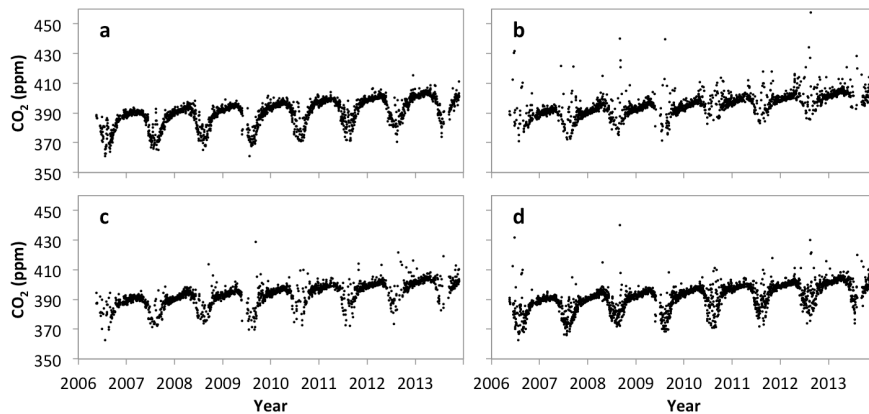


Fig. S2. Daily means after applying data selection to different hours of the day. The daily means were calculated from selected data of (a) daytime hours (1000–1500 LT); (b) nighttime hours (2200–0300 LT); (c) the transition hours (0500–0700 and 1700–1900 LT); and (d) the unselected whole hours of a day.

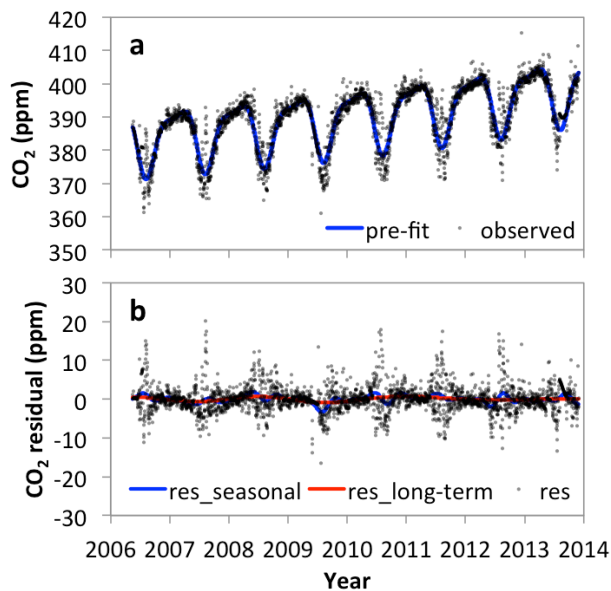


Fig. S3. Applying function fit and the low-pass filter to the dataset. The panels show the calculation procedures as follows: (a) the preliminary fit was calculated based on the daily means; (b) for the residuals of the daily means about the preliminary fit, low-pass filters were applied with cutoff frequencies of 120 days (seasonal) and 667 days (long-term).

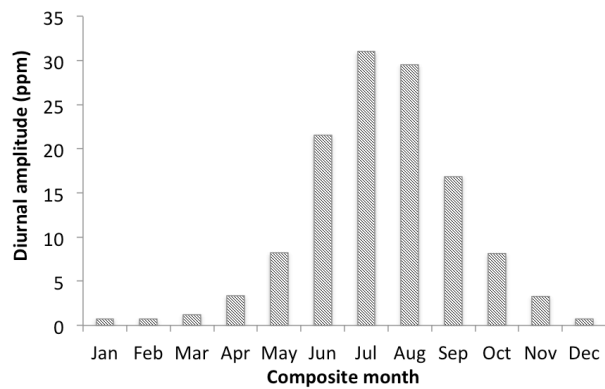


Fig. S4. Monthly means of diurnal CO₂ variation amplitude at Rishiri Island in 2006–2013.

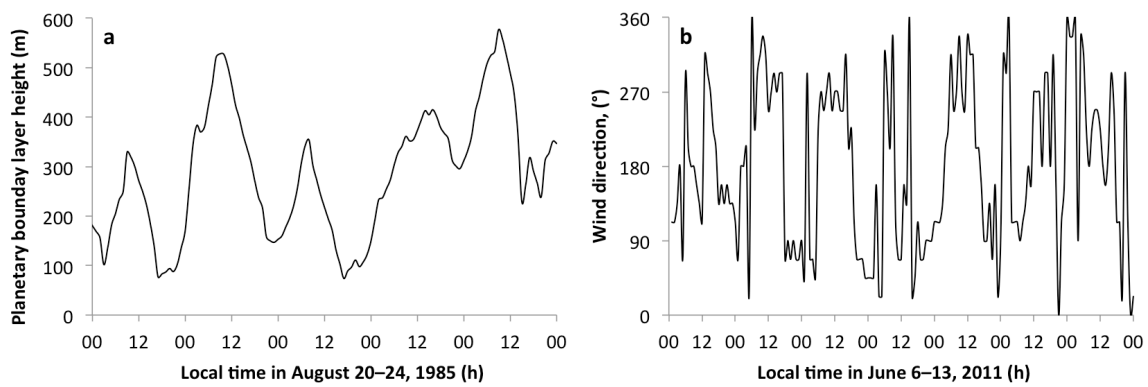


Fig. S5. Typical cases of diurnal variation of (a) planetary boundary layer height in August 20–24, 1985, during calm days; and (b) wind direction in June 6–13, 2011, showing the influence of the sea–land breeze and the mountain–valley airflow on the observation.

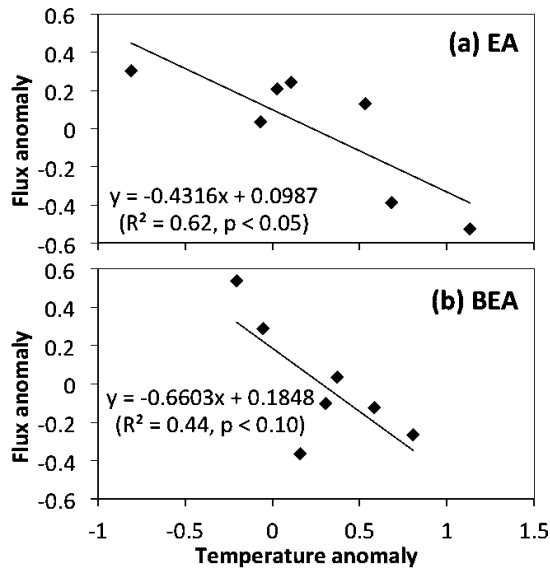


Fig. S6. Relations of temperature anomaly (means of current March to previous April) and flux anomaly (current year) in (a) East Asia and (b) broad East Asia.

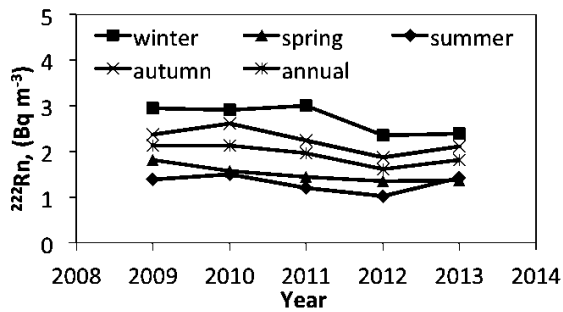


Fig. S7. The annual change in ^{222}Rn concentration at Rishiri Island in each season in 2009–2013.

References

Peterson, J. T., Komhyr, W. D., Harris, T. B., Waterman, L. S.: Atmospheric carbon dioxide measurements at Barrow, Alaska, 1973–1979, *Tellus*, 34, 166–175, doi: 10.1111/j.2153-3490.1982.tb01804.x, 1982.

- Peterson, J. T., Komhyr, W. D., Waterman, L. S., Gammon, R. H., Thoning, K. W., Conway, T. J.: Atmospheric CO₂ variations at Barrow, Alaska, 1973–1982, *J. Atmos. Chem.*, 4, 491–510, 1986.
- Thoning, K. W., Tans, P. P., Komhyr, and W. D.: Atmospheric carbon dioxide at Mauna Loa Observatory: 2. Analysis of the NOAA/GMCC data, 1974–1985, *J. Geophys. Res.* 94, 8549–8565, 1989.
- Brailsford, G. W., Stephens, B. B., Gomez, A. J., Riedel, K., Mikaloff Fletcher, S. E., Nichol, S. E., and Manning, M. R.: Long-term continuous atmospheric CO₂ measurements at Baring Head, New Zealand, *Atmos. Meas. Tech.*, 5, 3109–3117, doi:10.5194/amt-5-3109-2012, 2012.
- Haszpra, L.: On the representativeness of carbon dioxide measurements, *J. Geophys. Res.*, 104(D21), 26953–26960, doi:10.1029/1999JD900311, 1999.